Figure S1 Signal intensity changes over the respiratory (VENT) and cardiac (Perf) cycle at different positions within the parenchyma (left-top (L-T), left-middle (L-M), left-bottom (L-B), right-top (R-T), right-middle (R-M), and right-bottom (R-B) and noise regions (left-top (N-T-L), left-bottom (N-B-L), right-top (N-T-R), right-bottom (N-B-R). Frame 6 corresponds to end-expiration in the ventilation analysis, frame 7 corresponds to the end-systolic phase of the cardiac cycle in the perfusion analysis. For easier comparison, the data were normalized by the maximal ventilation and perfusion value. Noise data was additionally shifted by about 0.5 for better appreciation of shape differences within the lung parenchyma and noise regions.
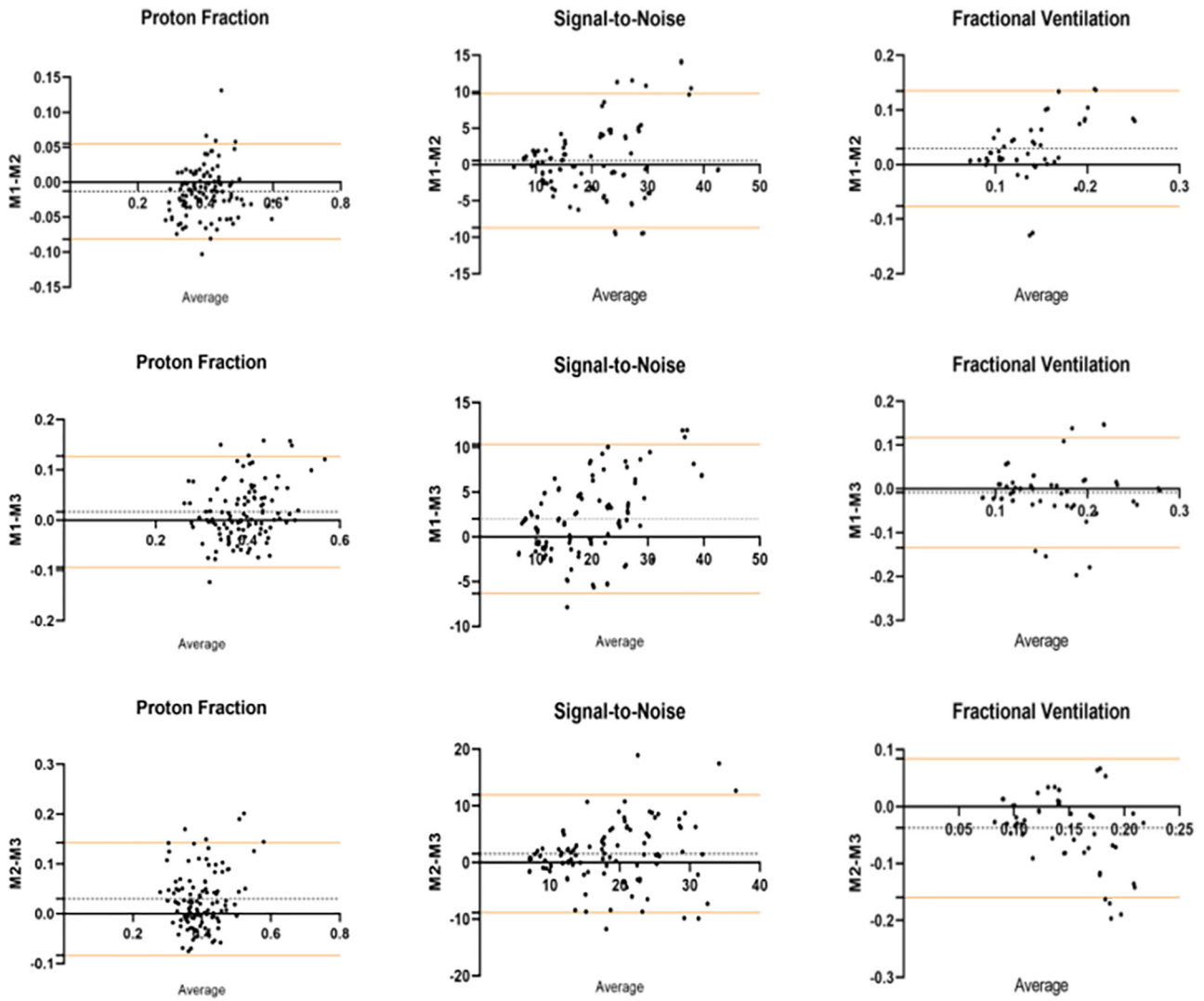
Figure S2 Bland-Altman analysis of the differences between the repeated measurements of lung density, signal-to-noise, and fractional ventilation derived from breath-hold data.
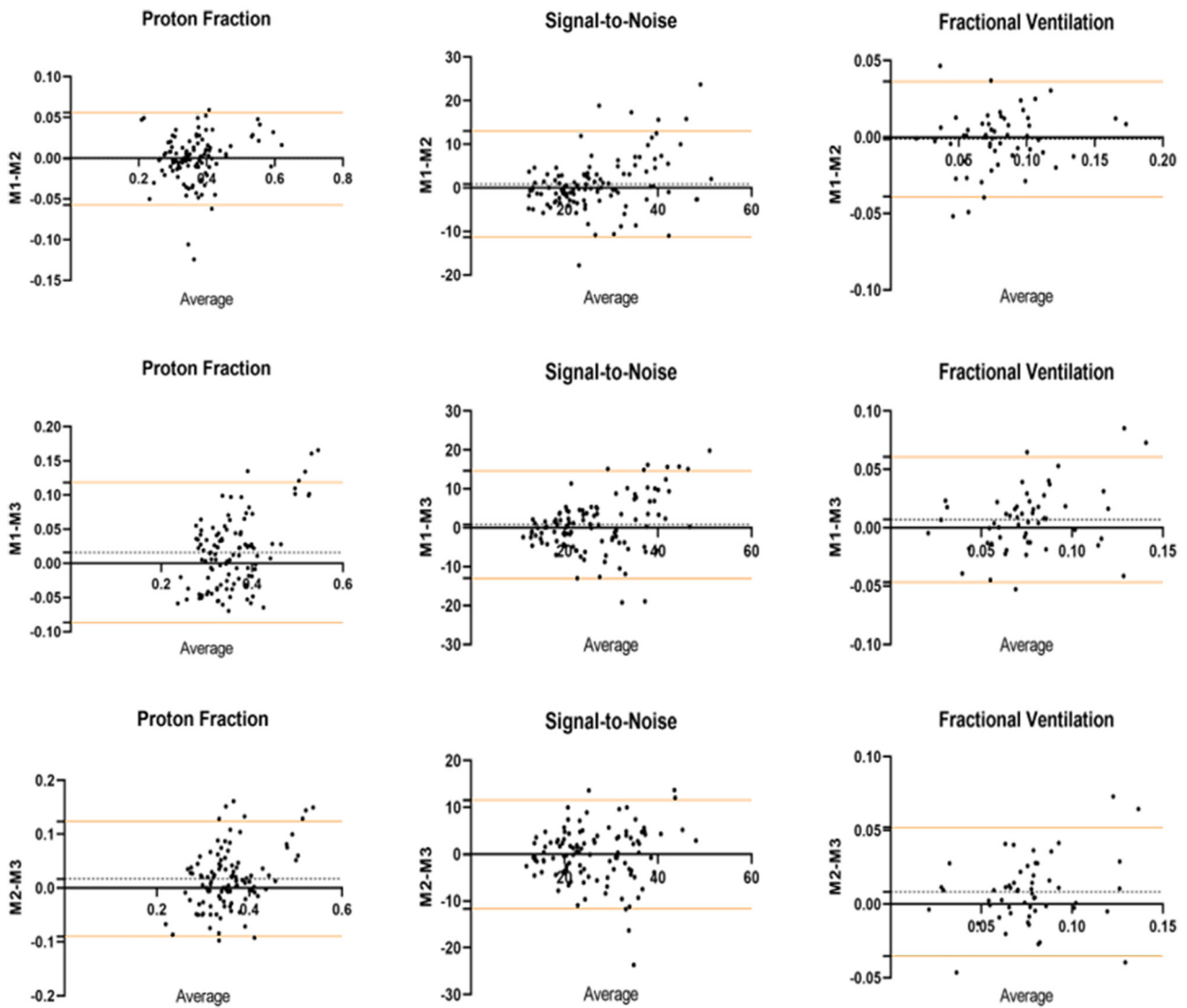
Figure S3 Bland-Altman analysis of the differences between the repeated measurements of lung density, signal-to-noise, and fractional ventilation derived from free-breathing data.
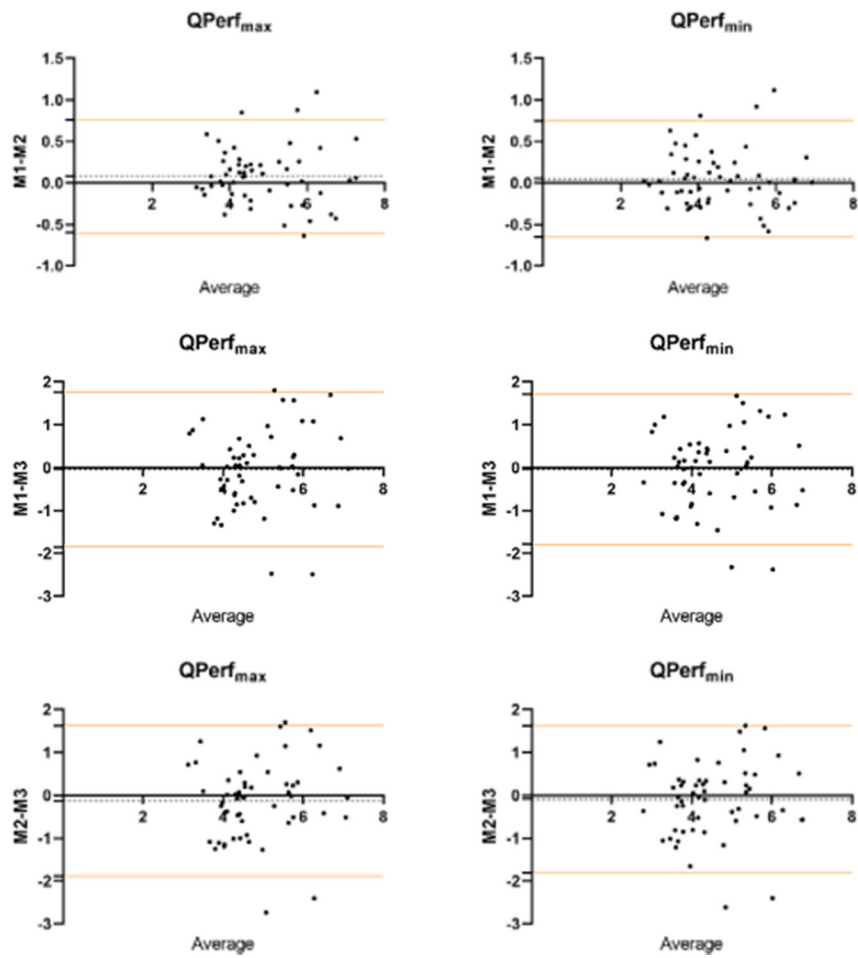
Figure S4 Bland-Altman analysis of the differences between the repeated measurements of lung density, signal-to-noise, fractional ventilation derived from free-breathing data. QPerfmax: maximum perfusion value over the cardiac cycle; QPerfmin: minimum perfusion value over the cardiac cycle.
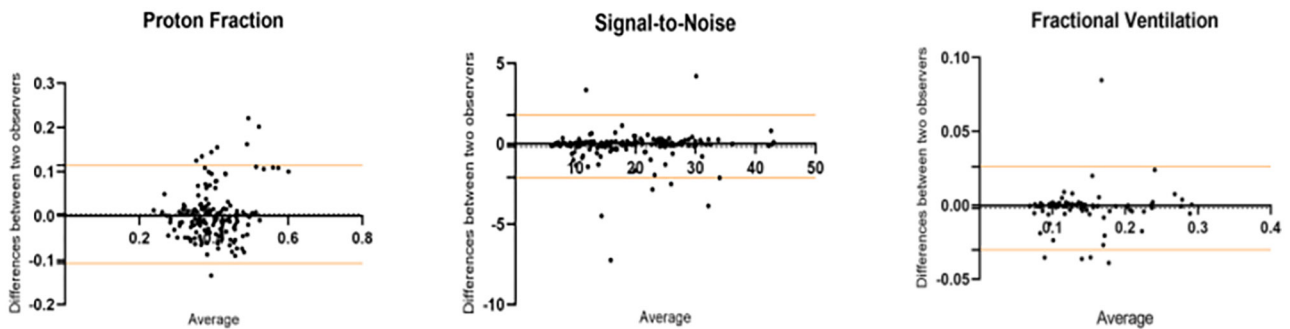

Figure S5 Bland-Altman analysis of the differences between the two observers for lung density, signal-to-noise, and fractional ventilation derived from breath-hold data.
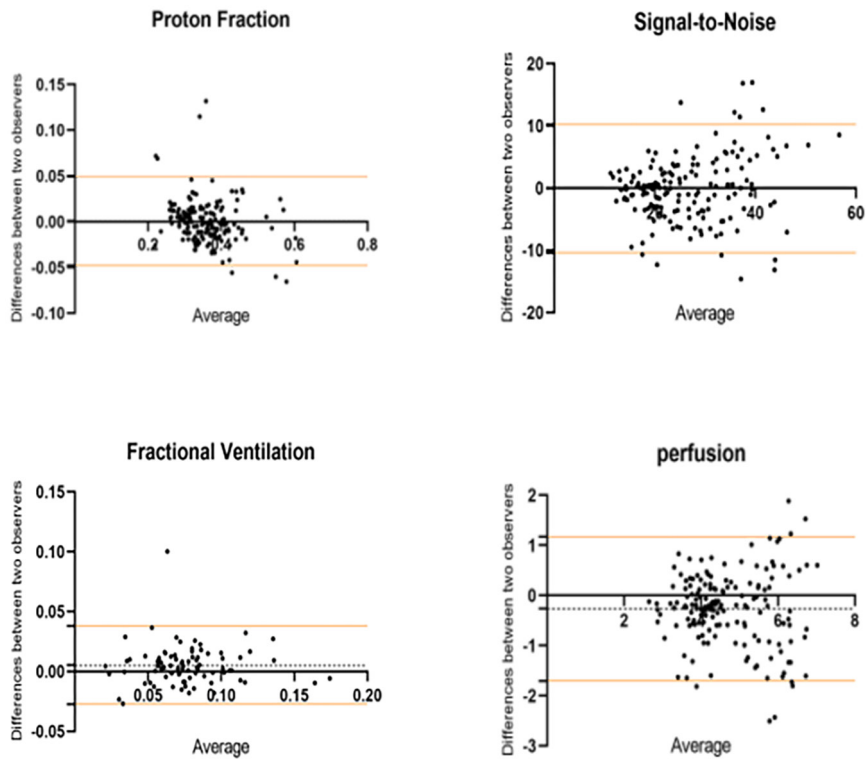
Figure S6 Bland-Altman analysis of the differences between the two observers for lung density, signal-to-noise, fractional ventilation and perfusion derived from free-breathing data.

Table S1 Intraclass correlation coefficient between the three free-breathing measurements

Parameters	Respiratory phase	M1 *vs.* M2	M1 *vs.* M3	M2 *vs.* M3
Lung density	EX	0.97 (0.95; 0.98)	0.82 (0.68; 0.89)	0.77 (0.60; 0.87)
	IN	0.96 (0.93; 0.98)	0.83 (0.70; 0.90)	0.80 (0.64; 0.88)
Signal-to-Noise	EX	0.87 (0.78; 0.93)	0.85 (0.75; 0.92)	0.89 (0.81; 0.94)
	IN	0.92 (0.87; 0.95)	0.85 (0.74; 0.91)	0.85 (0.74; 0.91)
Fractional ventilation		0.90 (0.82; 0.94)	0.70 (0.48; 0.87)	0.78 (0.60; 0.88)
$QPerf_{max}$		0.98 (0.96; 0.99)	0.78 (0.61; 0.87)	0.79 (0.64; 0.88)
$QPerf_{min}$		0.97 (0.86; 0.99)	0.80 (0.66; 0.89)	0.82 (0.68; 0.89)

Table S2 Intraclass correlation coefficient between the three breath-hold measurements

Parameters	Respiratory phase	M1 *vs.* M2	M1 *vs.* M3	M2 *vs.* M3
Lung density	EX	0.92 (0.87; 0.95)	0.69 (0.46; 0.82)	0.70 (0.47; 0.83)
	IN	0.81 (0.59; 0.90)	0.60 (0.40; 0.75)	0.66 (0.27; 0.83)
Signal-to-Noise	EX	0.82 (0.71; 0.89)	0.86 (0.75; 0.92)	0.83 (0.72; 0.90)
	IN	0.89 (0.81; 0.93)	0.81 (0.59; 0.91)	0.88 (0.71; 0.94)
Fractional ventilation		0.52 (0.16; 0.73)	0.58 (0.27; 0.75)	0.28 (0.14; 0.56)

Table S3 Structural similarity index of Fractional ventilation from BH of 3 measurements

Parameter	Slice	M1 *vs.* M2	M1 *vs.* M3	M2 *vs.* M3
Fractional ventilation	Anterior	0.94±0.02	0.85±0.03	0.85±0.03
	Middle	0.92±0.03	0.81±0.05	0.80±0.05
	Posterior	0.92±0.03	0.80±0.05	0.80±0.05

Table S4 Structural similarity index of fractional ventilation from FB of 3 measurements

Parameter	Slice	M1 *vs.* M2	M1 *vs.* M3	M2 *vs.* M3
Fractional ventilation	Anterior	0.92±0.04	0.84±0.02	0.84±0.02
	Middle	0.92±0.02	0.78±0.05	0.79±0.05
	Posterior	0.91±0.02	0.79±0.04	0.79±0.04

Table S5 Structural similarity index of ventilation and perfusion map (derived from spectral analysis)

Maps	Slice	M1 *vs.* M2	M1 *vs.* M3	M2 *vs.* M3
Ventilation map	Anterior	0.94±0.01	0.86±0.05	0.86±0.05
	Middle	0.91±0.02	0.79±0.06	0.79±0.06
	Posterior	0.89±0.03	0.78±0.06	0.78±0.06
Perfusion map	Anterior	0.92±0.02	0.84±0.03	0.85±0.04
	Middle	0.88±0.01	0.79±0.06	0.79±0.05
	Posterior	0.87±0.02	0.77±0.07	0.77±0.05

Table S6 Structural similarity index of Fractional ventilation and Spectral analysis from FB

Maps	Slice	M1	M2	M3
Fractional ventilation *vs.* spectral analysis	Anterior	0.88±0.03	0.88±0.03	0.88±0.03
	Middle	0.82±0.02	0.83±0.02	0.81±0.02
	Posterior	0.81±0.03	0.81±0.03	0.79±0.04